Quasiparticle properties of Fe, Co, and Ni

M. M. Steiner
Theoretical Division, Los Alamos National Laboratory, Los Alamos, New Mexico 87545
and Department of Physics, University of California at San Diego, La Jolla, California 92093-0319

R. C. Albers
Theoretical Division, Los Alamos National Laboratory, Los Alamos, New Mexico 87545

L. J. Sham
Center for Materials Science, Los Alamos National Laboratory, Los Alamos, New Mexico 87545
and Department of Physics, University of California at San Diego, La Jolla, California 92093-0319
(Received 6 December 1991)

For narrow electronic bands in metals, we seek improvement over the local-density approximation (LDA) by including the on-site Coulomb interaction between localized electrons. For the 3*d* ferromagnetic series of Fe, Co, and Ni, by treating fluctuations to second order in the on-site interaction around the LDA solution, in comparison with experiment a distinct improvement over the conventional LDA is obtained for a number of properties: effective masses, x-ray photoemission spectra, and results derived from angle-resolved photoemission spectra, such as exchange splittings and quasiparticle bands. In addition, the predicted quasiparticle broadenings and satellite features, which are not present in standard LDA calculations, are in reasonable agreement with observation.

I. INTRODUCTION

In this paper we extend our study of strongly correlated systems, where both on-site electron-electron interactions and hybridization are important, from model calculations[1] to real systems. As we shall see below, in this respect, there are many theoretical and experimental indications which suggest that the 3*d* transition-metal ferromagnets (Fe, Co, and Ni) are a particularly good choice to explore, since they are relatively simple systems where the interplay of these effects is important. A partially successful electronic-structure theory for these systems is that based on the local spin-density approximation to density-functional theory (LSDA-DFT),[2] which is in generally fairly good agreement with experiment for the ground-state properties of the 3*d* ferromagnets.[3–5] Unfortunately, however, within this theoretical framework there are some notable discrepancies for the excited-state properties, which tend to become more pronounced on going from Fe to Ni. Since the local-density approximation (LDA) gives a good exchange-correlation potential for the tetrahedral semiconductors,[6] we would expect at least part of these discrepancies to arise from causes other than the LDA's insufficient treatment of charge densities with strong spatial variations. The most likely failure in this case is the association of the eigenvalues of the Kohn-Sham equations with the quasiparticle energies, which is not only a poorer approximation than the one-electron Green's-function prediction for the quasiparticles, but also has no theoretical underpinning.[2] Furthermore, experiments show features such as satellite structure which *cannot* be explained within a one-electron picture. In this paper we will correct for these defects in the theory by treating the on-site Coulomb interaction of the 3*d* electrons in an approximation that goes beyond LDA and then evaluating the resulting one-electron Green's function.

The basic features of the electronic structure of Fe, Co, and Ni can be understood on the basis of their two types of valence-electron orbitals. On the one hand, extended 4*s* and 4*p* orbitals overlap to form broad free-electron-like bands. These orbitals should be well described by standard electronic-structure LDA techniques. On the other hand, the 3*d* orbitals are fairly well localized (about 90% of the atomic orbital lies within the Wigner-Seitz sphere), and in a solid form relatively narrow bands (of total width of about 5 eV), which are pinned to the Fermi energy and hybridize only weakly with the 4*s* and 4*p* bands. Because of the localized nature of these 3*d* states, the interaction between electrons in such orbitals gives rise to important dynamic 3*d*-3*d* correlation effects, which are not adequately dealt with in a one-electron picture. It is these narrow 3*d* bands that drive the magnetism in these systems. Within a Stoner model[7] for itinerant magnetism, which works well for the 3*d* ferromagnets, a spin moment develops if the gain in exchange energy is larger than the loss in kinetic energy. This magnetization leads to a nearly filled set of majority 3*d* bands, while the minority 3*d*-band filling increases from about two electrons in Fe to about four in Ni, and the spin moment decreases accordingly from 2.1 to 0.6.

As mentioned above, theory and experiment agree reasonably well for the ground-state properties of the 3*d* ferromagnets; i.e., lattice structure, lattice constants, and bulk moduli[3,8] are within the expected errors for elemental solids. Even the most serious discrepancy, the incor-

rect LSDA prediction for a fcc instead of the experimental bcc ground-state in Fe, is due to a tiny energy difference between the two structures. As better spin exchange-correlation potentials are used, they tend to push the results towards the correct ground state (see Ref. 9), although the most accurate full-potential calculations still fail to give the correct ground state (see Ref. 10). Also, both the spin moments μ_{spin} and the Fermi surface[4,5] agree well with experimental results. However, the associated quasiparticle properties, exchange splittings δE_{ex}, and the density of quasiparticle states at the Fermi level, which is a measure of the linear coefficient of the low-temperature specific heat γ, are found to be 10% to 50% off (see Table I). Related to this is the finding that the occupied $3d$ bandwidth $W_{d,\text{occ}}$ is predicted to be 30% too broad in Ni. On top of this, various angle-resolved photoemission spectroscopies[12,16] (ARPES's) show that there is considerable lifetime broadening of the quasiparticles, and valence-band x-ray photoemission spectroscopy[14,15] (XPS) shows that a satellite appears at about 6 eV below the Fermi energy in Ni, neither of which can be explained within a one-electron picture. The marked improvement for Cu with respect to Ni in the agreement between theory and experiment for the quasiparticle properties leads to the generally accepted opinion that the discrepancies in the $3d$ ferromagnets arise from correlation effects between the electrons in the *partially* filled $3d$ band, since Cu has an additional valence electron that essentially fills up the $3d$ band. A quantitative comparison of LSDA predictions and experiment is given in Table I.

In Ref. 1 we used a perturbative approach to treat the electron correlations in the one-dimensional periodic Anderson model, and obtained, for a wide range of electron properties, a better description of narrow-band systems than the one given by the mean-field approximation. The approach consisted of two steps. First, we solved the model within the mean-field approximation, which accounted for the average electron-electron repulsion in the localized orbital. Then we included fluctuations around this solution up to second order in U, which parametrized the direct on-site electron-electron interaction. For the $3d$ ferromagnets we use basically the same method, but, since we are dealing with real systems, we no longer use a simple nearest-neighbor tight-binding Anderson-lattice model, but instead obtain our mean-field "LDA" solution directly from an *ab initio* electronic band-structure calculation. This approach, besides being more realistic, also gives us a well-defined, orthogonal basis set to work with. In the next section we discuss our approach in more detail, in Sec. III we present our results, and we conclude in Sec. IV. In the rest of the present section we justify our use of perturbation theory, and summarize previously published work that used a similar approach.

Since U is not necessarily small, it is not obvious that a theory involving a low-order perturbation expansion in U is sufficient. However, because we expand in the fluctuations around the mean-field solution instead of directly in U, we ensure that the applicable range of our approach

TABLE I. A comparison of the theoretical and experimental quasiparticle properties of the $3d$ ferromagnets and Cu.

		LSDA	Experiment	Our results
μ_{spin}[a]	Fe	2.20	2.13	2.13
	Co	1.56	1.52	1.52
	Ni	0.60	0.57	0.57
δE_{ex} (eV)[b]	Fe	2.0, 1.4, 2.3	2.1, 1.4, 1.8	1.9, 1.6, 1.8
	Co	1.6	0.9	1.0
	Ni	0.6, 0.6	0.3, 0.2	0.40, 0.39
γ (mJ mol^{-1} K^{-2})[c]	Fe	2.53	3.11, 3.69	3.48
	Co	2.09	3.22, 3.71	3.74
	Ni	4.71	5.92, 6.38	6.10
	Cu	0.72	0.70, 0.70	
$W_{d,\text{occ}}$ (eV)[d]	Fe	3.6	3.3	3.7
	Co	4.3	3.9	4.3
	Ni	4.2	3.2	3.1
	Cu	3.3	3.0[e]	

[a] See Ref. 11.

[b] The exchange splitting is energy and k dependent. We give results for Γ_{25}, P_4, and H_{25} in Fe; Γ_{12} in Co; and near L_3 and X_2 in Ni. See Ref. 12.

[c] The experimental values have been corrected for the electron-phonon enhancement. The first value is with the calculated correction, and the second is with the suggested correction. See Ref. 13.

[d] See Ref. 14.

[e] See Ref. 15.

will extend beyond the small-U regime. Horvatic and Zlatic[17] have shown that results of this type of approach compare well with Bethe ansatz results for the symmetric Anderson model in the weak- and intermediate-coupling regimes, and are still reasonably accurate even in the strong-coupling regime. More recent quantum Monte Carlo calculations of the dynamic properties also indicate that this is the case.[18] For the periodic Anderson model, Ref. 1 found good agreement between quantum Monte Carlo and perturbative results for properties related to the total energy. Because the coupling strength for the $3d$ ferromagnets is in the weak to intermediate regime, one might therefore hope that the chances of success for a perturbative-fluctuation approach would be particularly good for these systems.

For real systems there have been only a number of related calculations, most of which have been for Ni, where the discrepancies are most prominent. Davis and Feldkampf[19] used the self-energy of a stationary, corelike hole to calculate the quasiparticle spectrum of holes in Ni. They found a narrowing of the $3d$ bands, but also a satellite feature that was too pronounced. Liebsch[20] applied a T-matrix series in U to determine the one-particle spectral density of states in Ni, and found that he could not simultaneously find quantitative agreement at low and high energies. Treglia, Ducastelle, and Spanjaard[21] used a degenerate Hubbard model and used second-order perturbation theory to study the $3d$ ferromagnets. Using a number of approximations, they found a narrowing of the band, but, again, overemphasized the satellite in Ni. One of the approximations was to take a momentum- and orbital-independent self-energy determined from a rectangular bare density of states. Comparison at certain k points with the results of Kleinman and Mednick,[22] who do not use the above approximations in calculating the self-energy, show that these approximations are reasonable for Ni. Jordan and Hoyland[23] have used the same form for the self-energy as Treglia, Ducastelle, and Spanjaard to calculate spin-resolved ARPES energy dispersion curves along the KX direction. By adjusting the Fermi energy they find good agreement with experiment for the low-energy quasiparticle near the X point. Kulikov *et al.*[26] have calculated the optical conductivity for chromium, in a scheme where the matrix elements appearing in the self-energy are approximated by the dipole matrix elements, and for the interaction strength they have used an effective Stoner parameter. In none of the above calculations are the $3d$ filling and the chemical potential determined self-consistently. Taranko, Taranko, and Malek[24] have tested the effects of self-consistency for paramagnetic Ni, and found that the satellite disappears. However, they used dressed propagators, whereas for consistency one should use simultaneously both the dressed propagators and dressed vertices, which yields qualitatively different results.[25] Nolting *et al.*[27] used a generalized Hubbard model, where exchange has also been included, to study the ferromagnetism of Ni. By neglecting all spin-independent terms and making an atomiclike two-pole ansatz for the Green's function they obtained very impressive agreement for the temperature dependence of the magnetic moment and static susceptibility.

II. METHOD OF CALCULATION

We use the self-consistent LDA solution of a linearized-muffin-tin-orbital (LMTO) band-structure calculation as our starting point; details are given in Appendix A. This gives us an explicit orthonormal basis to work in, which is needed in our approach. In the LMTO method only a small basis set on each atom is usually needed to describe the valence electrons. Thus, the $3d$ ferromagnets are well described by an s-p-d basis, and, for convenience (see below), we use a cubic harmonic description of the angular part. The eigenvalues $\epsilon_{j\mathbf{k}\sigma}$ and the orthogonal eigenvectors $\tilde{\Psi}^L_{j\mathbf{k}\sigma}$ of the self-consistent LMTO calculation fully characterize the mean-field Hamiltonian, where j is a band index, $\mathbf{k}$ is a crystal momentum vector, σ is a spin index, and $L=\{\ell,m\}$, with ℓ an angular quantum number and m a cubic harmonic index. With this notation the mean-field Hamiltonian is

$$H^{\mathrm{MF}}_{\mathbf{k}\sigma}=\sum_j \epsilon_{j\mathbf{k}\sigma}|\tilde{\Psi}_{j\mathbf{k}\sigma}\rangle\langle\tilde{\Psi}_{j\mathbf{k}\sigma}| \ . \tag{1}$$

Because a mean-field treatment of the electron-electron interaction between two $3d$ electrons is not considered sufficient, we have separated out this term from the general electron-electron interactions and have treated it to higher order. It has the form

$$\sum_{\substack{i,\sigma,\sigma'\\ m_1,m_2\\ m_3,m_4}} U_{m_1,m_2;m_4,m_3} d^+_{i,m_1,\sigma} d^+_{i,m_2,\sigma'} d_{i,m_3,\sigma'} d_{i,m_4,\sigma} \ ,$$

where $d^+_{i,m,\sigma}$ creates a $3d$ electron on site i in the $\{m,\sigma\}$ d orbital. Of all the possible $3d$-$3d$ interactions we only keep two sets [see Fig. 1(a)]: (a) the $m=m_1=m_4$ and $m'=m_2=m_3$ terms, whose coefficient we call U, see the Appendix in Ref. 22, and (b) the $m=m_1=m_3$ and $m'=m_2=m_4$ terms, for $m\neq m'$, whose coefficient we denote by J. This reduces the more complete term given above (and after dropping the site index) to

$$U\sum'_{\substack{\sigma,\sigma'\\ m,m'}} n_{m,\sigma}n_{m',\sigma'} - J\sum_{\substack{\sigma,\sigma',m,m'\\ m\neq m'}} d^+_{m,\sigma}d_{m',\sigma}d^+_{m,\sigma'}d_{m',\sigma'} \ ,$$

where the prime in $\sum'$ indicates the restriction $\{m,\sigma\}\neq\{m',\sigma'\}$. The J term generalizes our previous work[1] to include exchange terms, which are essential to treat for magnetic systems.

The mean-field solution is most conveniently found in the basis that diagonalizes the local-density matrix,[30] which is the cubic harmonics in our case. Since we have chosen to start from a paramagnetic LMTO-ASA calculation, our mean-field occupations per site $\langle n_{m,\sigma}\rangle_{\mathrm{MF}}$ are spin and orbital independent. Because the mean-field contribution of the $3d$-$3d$ interaction has already been included in the LMTO calculation, we are left with a term representing the fluctuations in the $3d$ occupation numbers around their mean-field values. It is these fluctuations that are large enough to require more than just a mean-field treatment of the $3d$-$3d$ interactions, and are dealt with in the second step.

We go beyond mean field by treating these fluctuations

perturbatively, calculating the self-energy $\Sigma^{dd}_{\mathbf{k},\sigma}$ up to second order in U and J, and then including the resulting dynamical 3d-3d correlations by solving the Dyson equation for the full Green's function $\mathbf{G}_{\mathbf{k},\sigma}$, see Fig. 1(b):

$$[\tilde{\omega} - \mathbf{H}^{\mathrm{MF}}_{k} - \mathbf{\Sigma}_{\mathbf{k},\sigma}(\tilde{\omega})]\, \mathbf{G}_{\mathbf{k},\sigma}(\tilde{\omega}) = \mathbf{1}\,, \tag{2}$$

where $\tilde{\omega} = \omega - \mu + i\delta$, ω denotes the energy dependence ($\hbar = 1$), μ is the chemical potential, and δ is a positive infinitesimal to give the proper boundary conditions for a retarded Green's function. The mean-field Hamiltonian $\mathbf{H}^{\mathrm{MF}}_{k}$ is obtained from a paramagnetic LMTO-ASA calculation. The basis set for $\mathbf{G}_{\mathbf{k}}$ is 3d, 4s, and 4p, as described in Appendix A. The form of $\mathbf{\Sigma}_{\mathbf{k},\sigma}(\tilde{\omega})$, which is similar to that used in Ref. 1, see Fig. 1(c), is

$$\mathbf{\Sigma}^{dd}_{\mathbf{k},\sigma}(\omega) = \mathbf{\Sigma}^{(1)\ dd}_{\sigma} + \mathbf{\Sigma}^{(2)\ dd}_{\mathbf{k},\sigma}(\omega) - \Sigma^{dd}_{c}\,. \tag{3}$$

The first-order contribution $\mathbf{\Sigma}^{(1)\ dd}_{\sigma}$ is energy independent, real, and (by the choice of basis) diagonal; it can be written as $\Sigma^{(1)\ mm}_{\sigma} = \sum'_{m',\sigma'}(U + J\delta_{\sigma,\sigma'})\delta n_{m',\sigma'}$, where $\delta n_{m,\sigma} = (\langle n_{m,\sigma}\rangle - \langle n_{m,\sigma}\rangle_{\mathrm{MF}})$ and $\langle n_{m,\sigma}\rangle$ is the number of $\{m,\sigma\}$ electrons in the fluctuating state [see Fig. 1(d)]. This linear term in U and J allows for both spin and orbital polarization (i.e., the 3d occupation numbers can depend on both spin and the m orbital) and can be considered a correction to the paramagnetic spherically averaged LMTO-ASA one-electron $\{m,\sigma\}$ energy, since the average number of $\{m,\sigma\}$ electrons in the fluctuating state is not necessarily equal to those in the LMTO-ASA calculations. The dynamic correlations are dealt with in the second-order term $\mathbf{\Sigma}^{(2)\ dd}_{\mathbf{k},\sigma}(\omega)$, see Figs. 1(e) and 1(f). Details of its form and how we calculate it are presented in Appendix B. The fluctuating spin- and orbital-polarized value of $\langle n_{m,\sigma}\rangle$ is also used in the propagators for the second-order self-energy. The third term in Eq. (3), which is U and J independent, was not present in Ref. 1. It is necessary to prevent double counting of the 3d-3d correlations, since they are already partially included in the LDA solution through the exchange-correlation potential.

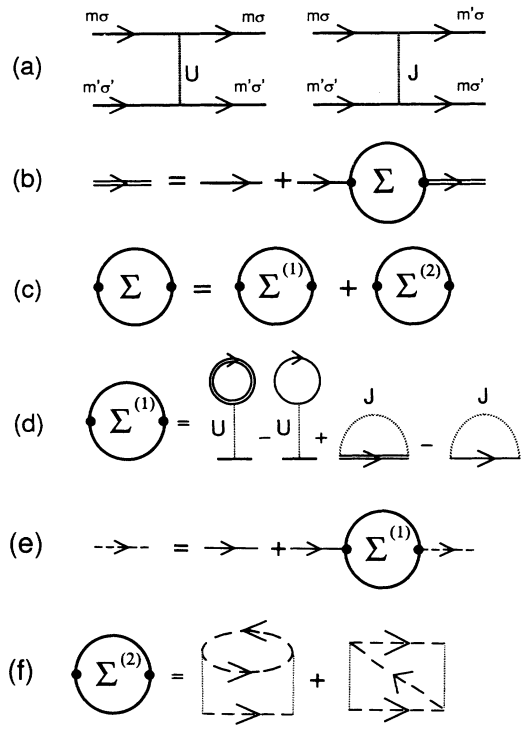

FIG. 1. (a) The two types of 3d-3d interactions that we keep, where for the J diagram we have the restriction $m \neq m'$ (m, m' are cubic harmonic indices and σ, σ' spin indices). (b) The diagrammatic form of the Dyson equation, Eq. (2). The single line represents the paramagnetic LMTO-ASA propagator, while the double line is the "full" Green's function. (c) The two nonvanishing terms of Eq. (3). (d) The first order in U and J term, see text below Eq. (3). Note that the mean-field result has to be subtracted in first order. (e) The broken single line represents a ferromagnetic propagator that has been corrected from the LDA values for the correlated system's fillings. (f) The second-order self-energy, where any of the vertical dotted lines can be either U or J.

A fully *ab initio* calculation would not only involve calculating $\mathbf{H}^{\mathrm{MF}}_{k}$, but also Σ^{dd}_{c}, U, and J as well. We have tried a number of schemes to calculate Σ^{dd}_{c}. For example, one might naively try $\Sigma^{dd}_{c} = \int \varphi^2(r) v_c[n_d(r)] r^2 dr$, where $\varphi(r)$ is the $\ell = 2$ LMTO radial wave function, $n_d(r)$ the total 3d charge density, and $v_c[n(r)]$ the correlation part of the exchange-correlation potential. For this purpose the von Barth–Hedin approximation to the exchange-correlation potential is particularly suitable, since the exchange and correlation terms can be readily separated. This gives about -2 eV for Σ^{dd}_{c}, which is larger than expected due to the nonlinear density dependence of $v_c[n(r)]$; this must be treated correctly, since the 3d charge density strongly overlaps with the 3p and 3s core orbitals in the core region and with the 4s and 4p charge density near the muffin-tin radius. To possibly better handle this nonlinearity, another estimate is given by $\Sigma^{dd}_{c} = \int \varphi^2(r)\{v_c[n(r)] - v_c[n(r) - n_d(r)]\} r^2 dr$, where $n(r)$ is the total charge density. This gives values of the order -0.1 eV, in agreement with a third possibility $\Sigma^{dd}_{c} = \int \varphi^2(r) \tilde{v}^{(U)}_{c}[n_d(r)] r^2 dr$, where $\tilde{v}^{(U)}_{c}(n)$ is the free-electron limit of $\Sigma^{(2)}(\mu)$, where the propagators are now those of free electrons, and the electron-electron interaction is U. Note that the last possibility, which requires introducing an ultraviolet cutoff to prevent the result from diverging, exactly cancels $\Sigma^{(2)}(\mu)$ in the limit of slow density variations. Since $\Sigma^{(2)\ dd}(\mu)$ is positive while Σ^{dd}_{c} is small but negative for the 3d ferromagnets, we have chosen to set it equal to zero for simplicity.

The problem of calculating U, which is the screened interaction between two mean-field 3d electrons, has received much attention recently.[31–33] Because there is no satisfactory *a priori* derivation of the Hubbard model, it is not completely clear how to calculate this quantity and which of the many different methods is best or most accurate. Difficulties arise from knowing how to correctly define the localized orbital, take care of screening effects, and handle hybridization. In our case we obviously want screening effects from all orbitals outside

TABLE II. U for the $3d$ ferromagnets, which are determined by various methods (see the text for a full description). All values are given in eV.

	U^{atomic}	$U^{(1)}$	$U^{(2)}$	U^{exp}	U	J	$\frac{U+4J}{5}$ (I)
Fe	2.0	3.0	5.0	1.0	1.2	0.73	1.03 (0.96)
Co	2.1	3.5	5.0	1.2	2.4	0.50	1.10 (1.01)
Ni	2.4	3.9	5.4	4.0	3.7	0.27	1.20 (1.03)

the minimal basis set (i.e., from higher ℓ and principal quantum number values). We also want to account for purely $4s$ and $4p$ screening, as well as $4s$-$3d$ and $4p$-$3d$ screening. One could argue that U should also be further renormalized by the $3d$-$3d$ screening not accounted for by $\Sigma^{(2)\,dd}_{\mathbf{k}\sigma}$, i.e., higher-order RPA-like terms. One proposed method is to downfold the system all the way onto a single-orbital ($3d$) Hubbard model, and then, by taking the atomic limit, to equate U with d^2E/dn_d^2, where E is the total mean-field electronic energy of the system. If this approach is applied to an isolated atom, one obtains the values U^{atomic} for the $3d$ ferromagnets that are given in the first column of Table II; they agree well with other similar atomic calculations.[34] For local-density-approximation calculations it can be shown that U can be equivalently calculated from $d(\epsilon_d-\epsilon_s)/dn_d$,[35] where ϵ_d and ϵ_s are the one-electron eigenvalues for the $3d$ and $4s$ orbitals, respectively. Performing the same type of calculation in the solid is usually done by using a constrained form of DFT.[36] In this approach a set of Lagrange parameters is added to constrain different types of occupation numbers, such as, for the $3d$ states (however, the total number of electrons is still usually constrained to maintain overall charge neutrality). The total energy or various eigenvalues are monitored as a function of these occupation numbers (in the otherwise self-consistent calculations), from which in turn U is computed. The second column of Table II gives results for U calculated in the constrained solid by the same (atomic) formula $U^{(1)} = d(\epsilon_d-\epsilon_s)/dn_d$. However, since calculations for the U in solids have often used a different formula such as $d\epsilon_d/dn_d$ or $d(\epsilon_d - E_f)/dn_d$, where E_f is the Fermi energy,[37] we have additionally tabulated results using the first of these two formulas in column 3, listed as $U^{(2)}$. This gives results larger than one would expect for good metals, while the second of the formulas gives even larger values for U. To provide an idea of what governs U, an oversimplified picture (i.e., a $3d$ and $4s$ two-orbital atomic-limit Hubbard Hamiltonian for $3d$ atoms) is that $d(\epsilon_d-\epsilon_s)/dn_d$ gives $U = U_{dd}-2U_{sd}+U_{ss}$, while $d\epsilon_d/dn_d$ gives $U = U_{dd} - U_{sd}$.[35] In the constrained solid-state calculations we have included many hybridization effects in the total energy, and therefore in U, which means that they are partially double counted, if they also appear in the model Hamiltonian as one-electron hopping terms. Hybertsen, Schlüter, and Christensen,[31] McMahan, Martin, and Satpathy,[32] and Gunnarson *et al.*[33] have developed methods to prevent this. We have performed calculations similar to these methods, and find for the $3d$ ferromagnets at most a 0.7-eV difference from the values from the more straightforward method tabulated in column 3. In the fourth column in Table II we quote experimental values U^{exp}, which were obtained from an analysis of Auger spectra.[38]

If we substitute the above computed values of U in our second-order fluctuation theory, we find that the values of U are too large to give good agreement with experimental results. [In this context we mention, as pointed out by Anisimov, Zaanen, and Andersen,[30] that the LDA+U approach, which they successfully used for the Mott insulators, breaks down for the $3d$ ferromagnets. (The "LDA+U" approach is equivalent to just keeping the first-order term for the self-energy in our approach.) The main reason for this breakdown is that the constraint density-functional theory values of U and J for the $3d$ ferromagnets are too large. As a result one finds large changes in the charge density, quasiparticle dispersion, and Fermi surface with respect to the standard LDA, which are not reflected by experiments. Further, this type of approach does not take into account the dynamic correlations, which we find to be important.] We have therefore used empirical values for U and J, chosen to give (a) the experimental magnetic moment, and (b) the best agreement between the experimental XPS result and the total density of states. These empirical values for U and J are given in columns 5 and 6 of Table II, respectively. Within a mean-field picture and after spherical averaging, $(U+4J)/5$ is equivalent to the Stoner exchange parameter I, which we have calculated using the method proposed by Gunnarsson;[7] these values are compared in column 7 of Table II. Although the values for U from constrained DFT are too large for the $3d$ ferromagnets (for instance, a 5-eV value for U would produce a very large orbital polarization in Fe, which is not observed), it is interesting to note that both they and the Stoner parameter I are nearly the same for Fe, Co, and Ni. This is what one would intuitively expect, since the shape of the $3d$ orbital does not change very much between Fe, Co, and Ni. On the other hand, both our phenomenological values of U and J, and U^{exp}, which are in relatively good agreement, vary considerably. We are investigating whether multiple intrasite scattering can account for this variation from Fe to Ni.

III. RESULTS

In order to understand our results it is useful to first discuss the changes that the individual terms of the self-energy [see Eq. (3)] can produce with respect to the LDA results. The main effect of the first term is to give rise to magnetism by splitting the paramagnetic bands into majority and minority bands, as in a Stoner description of

magnetism. Orbital polarization is also allowed (i.e., the occupation numbers can depend on m, the orbital quantum number); however, for the $3d$ ferromagnets, which have reasonably close-packed structures, we would expect this effect to be small, especially given the size of U and J. Additionally, an overall shift of the $3d$ bands with respect to the $4s$ and $4p$ bands is possible if the total $3d$ occupation is different from its LDA value. In the second term of Eq. (3) we go beyond a one-electron picture. The energy dependence of the real part of $\Sigma^{(2)\,dd}_{\mathbf{k},\sigma}(\omega)$ can change the $3d$ bandwidth, renormalize the band masses, further shift the $3d$ bands with respect to the other bands, and cause additional features (i.e., satellites) to appear, while the imaginary part of $\Sigma^{(2)\,dd}_{\mathbf{k},\sigma}(\omega)$ gives the quasiparticles a nonvanishing lifetime due to electron-electron scattering. The average shift of the first-order term always opposes the average shift of the second-order term, which leads to a stable self-consistent solution. This is a result of determining μ and $\delta n_{m,\sigma}$ consistently with the total number of electrons and $\langle n_{m,\sigma}\rangle$, which is necessary (cf. the discussion in Ref. 1). Details of this calculation and the LMTO-ASA calculations are presented in Appendixes A and B. [Note that the third term in Eq. (3) is a small double-counting correction that we have found negligible.]

Table III, where we list values for the chemical potential μ and the change in $3d$ occupations relative to the band-structure values $\delta n^{3d} = \sum_{m,\sigma} \delta n_{m,\sigma}$, gives some indication of the relative changes caused by the fluctuation terms. Most of these results follow from the upwards shift of the $3d$ bands, due to the positive spin, orbital, and momentum average of the real part of the self-energy. This causes μ to also move upwards in order to preserve the total electron count. As shown in Table III, this effect becomes stronger as one passes from Fe to Ni. On the other hand, the broad $4s$ and $4p$ bands do not shift, and so there is a small transfer of electrons from the $3d$ states to the $4s$ and $4p$ states. The smallness of δn^{3d} shows that the fluctuation theory does not change the occupation numbers very much away from the LDA values; this provides additional (*a posteriori*) justification for using the paramagnetic LMTO-ASA results as the starting point for our calculations. Since the chemical potential is shifted by approximately the same amount as the $3d$ bands, the changes in the predominantly $3d$ parts of the Fermi surface, with respect to the LDA Fermi surface, are small. Because the $4s$ and $4p$ bands are relatively steep near the chemical potential, changes in the corresponding parts of the Fermi surface are also small.

TABLE III. The second-order fluctuation theory results for the chemical potential μ, and the change δn^{3d} in the $3d$ occupations relative to the band-structure results.

	μ (eV)[a]	δn^{3d}
Fe	−1.01 (−1.01)	−0.013
Co	−0.74 (−1.05)	−0.035
Ni	−0.84 (−1.35)	−0.050

[a] The results in parentheses are from the paramagnetic LMTO-ASA calculation.

Since LDA band-structure techniques usually give good results for ground-state properties, such as partial occupation numbers and the Fermi surface, it is satisfying that our improved treatment of correlation effects does not produce large changes in these properties.

In making this comparison it is important to keep in mind the possible sources of error. In the LMTO-ASA calculations these include the neglect of spin-orbit relativistic effects, the use of spherical averaging and atomic-sphere overlap method instead of a full-potential method, and the local-density approximation to density-functional theory. These errors are carried over into our results. Note also that our starting point is paramagnetic rather than ferromagnetic.[39]

Even though our method of empirically determining U and J ensures that we obtain good agreement with experimental and LSDA spin moments as well as between XPS data and the total occupied density of states (DOS), it is instructive to compare our results with the corresponding LSDA results. In Fig. 2 we show how U and J are empirically determined for Fe by comparing the XPS data of Kirby *et al.*[14] (the bottom curve) with the results for the total occupied DOS for various U and J values, under the constraint that the calculated spin moment agrees with experiment. We see that the quasiparticle features become less pronounced with increasing U, and above 1.6 eV a satellite appears, which becomes more pronounced on further increasing U. Höchst, Goldmann, and Hüfner[14] have reported a weak satellite; however, the more recent experiments by Kirby *et al.* have not confirmed this. We have chosen $U = 1.2$ eV and $J = 0.73$ eV, corresponding to Fig. 2(d), which gives reasonably good agreement with the XPS data. In making all of these comparisons note that we have folded in the quoted instrumental resolution, which corresponds to a full width at half maximum of 0.7 eV. Other sources of er-

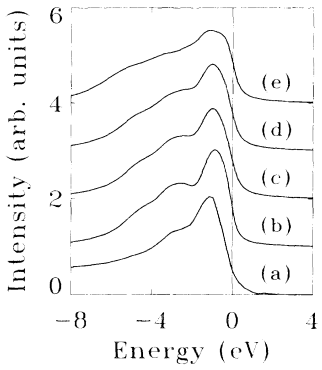

FIG. 2. A comparison of the XPS for Fe with the calculated total occupied DOS for different values of U and J (in eV): (a) experiment (Ref. 14); (b) $U = 0.0, J = 1.03$; (c) $U = 0.95, J = 0.80$; (d) $U = 1.22, J = 0.73$; (e) $U = 1.91, J = 0.62$. The energies have been shifted so the Fermi energy is at zero energy. An instrumental resolution corresponding to that of the experiments (full width at half maximum = 0.7 eV) has been folded into the calculated curves.

rors in making these comparisons between photoemission data and the DOS arise from the neglect of the energy and angular momentum dependence of matrix elements, surface effects,[15] and the energy dependence of lifetime broadening.

The three curves from the top to the bottom of Figs. 3(a)–3(c) show, respectively, the ferromagnetic LMTO occupied DOS, our results, and the experimental XPS for Fe, Co, and Ni. Note that the appropriate experimental broadening has been folded into the theoretical results. In each of the three different cases the LMTO band calculations produce structure that is too prominent relative to experiment. Finite quasiparticle lifetime effects (discussed later in this section) broaden our fluctuation theory results and bring them into better agreement with the experimental results. In addition, we pick up the satellite structure near -6 eV in Ni.

In Fig. 4 we show our results for the *unbroadened* spin-resolved total DOS. As mentioned earlier, the majority spin states (solid line) are almost completely occupied for all three ferromagnets, while the minority spin states (dotted line) are increasingly filled when going from Fe to Ni. The characterization of the results depends both on this filling and on the relative strength of U.

For Fe, which of the $3d$ ferromagnets has the smallest value for U and the largest value for J, the dominant quasiparticle shifts come from the spin-polarization term of $\Sigma^{(1)}$, which depends on the effective Stoner parameter $I = (U + 4J)/5$. Because U is small, orbital polarization is negligible, and further quasiparticle shifts due to $\Sigma^{(2)\,dd}_{\mathbf{k},\sigma}(\omega)$ are correspondingly small. The main effect of the second-order term is to broaden the quasiparticles by including lifetime effects due to the $3d$-$3d$ electron-electron interaction. Although these lifetime effects are proportional to U^2, the imaginary part of the self-energy is also proportional to the number of possible particle-hole excitations, which is large in Fe because of the only partially occupied minority band. This compensates for the relatively smaller U.

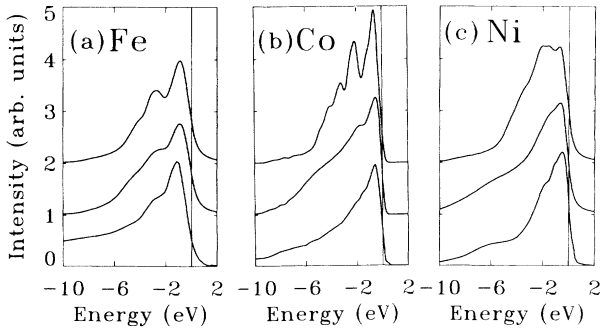

FIG. 3. The XPS for (a) Fe, (b) Co, and (c) Ni compared to the total occupied DOS. The three curves from the top to the bottom of each figure show, respectively, the ferromagnetic LMTO occupied DOS, our results, and the experimental XPS. In each case the quoted experimental broadening has been folded into the theoretical results. The energies have been shifted so the Fermi energy is at zero energy.

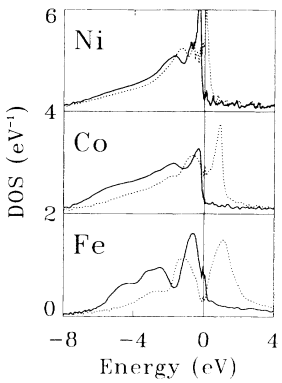

FIG. 4. The unbroadened spin-resolved DOS for the $3d$ ferromagnets (solid/dotted line = majority/minority states). (The noise in the tails is due to the discretization of momentum space.) The energies have been shifted so the Fermi energy is at zero energy.

The U and J in Co are in between those of Fe and Ni, as are most of the results such as the spin polarization (which is mostly determined by J). Because U is still somewhat small, orbital polarization is also correspondingly small. Lifetime effects are somewhat suppressed relative to Fe, because the small increase in U is offset by the decrease in the number of minority-state holes. Note that the small shoulder in Co near -5.5 eV is *not* a satellite, but arises from hybridization between the majority $4s$ and $3d$ bands.

For the larger-U (3.7-eV) case of Ni, in addition to the spin-polarization term there is also a small orbital-polarization contribution to $\Sigma^{(1)}$, as well as important dynamic-correlation effects arising from $\Sigma^{(2)}$. These effects include narrowing of the $3d$ bands, which LSDA predicts to be too broad (cf., the Introduction and Table I). Another way of expressing this is that U reduces the effective hopping from its mean-field value, because electron hopping costs additional energy arising from changes in the local $3d$-occupation number. The resulting weak correlations lead to a slightly correlated quasi-mean-field state, which for larger U would become a Kondo-like lattice state. Besides the narrowing, U also causes a broad dispersionless satellite to appear at about -6 eV, which reflects a $d^9 \rightarrow d^8$ local atomiclike excitation; on further increasing U this would separate from the main $3d$ band and become a narrow atomiclike state. Thus, in Ni, both quasi-mean-field and pseudoatomic excitations are present.

Besides comparing k-summed DOS with XPS, we can also compare k-resolved DOS with angle-resolved photoemission spectroscopy (ARPES) and the inverse process, IARPES. Here, one must remember that the experimental analysis is often difficult, requiring background subtractions and deconvolutions of broad overlapping peaks; also, spurious features can arise from surface states and adsorbates. While the older ARPES data sets are more complete than the newer spin-resolved ARPES data, they have often been at variance with one another (see the note added in proof in Ref. 22), which makes a compari-

son of our results with the older data difficult.

In Figs. 5(a) and 5(b) we show the k-resolved DOS for the H point in Fe and the X point in Ni. Well-defined peaks in the theoretical DOS correspond to predicted quasiparticles; the corresponding experimental peaks (when available) are indicated by the thick vertical lines on the abscissa. While the quasiparticles above the Fermi energy at the H point compare well with the recent IARPES results of Santoni and Himpsel,[12] those below do not agree well with the ARPES results of Turner, Donoho, and Erskine.[12] We believe that this is most likely due to the use of free-electron bands in the energy-momentum relationship for the outgoing electrons in the experimental ARPES analysis. For example, band-structure calculations[4] give $E(H_{15})$ to be about 10 eV, while the free-electron band value used was about 14 eV; the later experiments of Santoni and Himpsel[12] found good agreement with the band-structure value. In Fig. 5(b) the lower two thick lines near -3 eV represent ARPES data of Eberhardt and Plummer[16] for Ni. An odd and even analysis of the off-normal ARPES made it possible to distinguish between the X_1 (the lower line) and X_3 (the upper line) symmetry. However, because the experiment was not spin resolved, no separation into majority and minority components is possible. The states do not seem to be good quasiparticles in our calculations, since they are very broad smudges (much like the ARPES data), and we have not attempted to resolve them into quasiparticle peaks, even though it is possible for us to do the same odd/even analysis. The upper two thick vertical lines (near the Fermi energy) are the majority (lower line) and minority (upper line) X_2 quasiparticles found in the spin-resolved ARPES of Raue and Hopster.[12] Although LSDA electronic-structure methods consistently put the minority X_2 point slightly above the Fermi energy, de Haas–van Alphen[4,5] data agree with the spin-resolved ARPES in placing it slightly below. In our calculations the majority peak (solid line) just below the Fermi energy is a superposition of X_2 and X_5 states. We resolve the minority component (dotted line) of these states: the X_2 minority quasiparticle is slightly below the Fermi energy (in agreement with the spin-resolved ARPES and de Haas–van Alphen data), and the X_5 minority quasiparticle is slightly above. The majority-state peak that is about 3 eV above the Fermi energy is an unrelated p state. Note that the good agreement with experiment for the minority X_2 quasiparticle is a result of *not* averaging t_{2g} and e_g occupation numbers. Because of the diffuse nature and lack of spin resolution of the states at lower energies, it is hard to know what to make of the discrepancy between our calculation and the data. The experimental analysis also used free-electron bands in their analysis.

Our results for the exchange splittings $\delta E_{\rm ex}$ are presented in Table I. When compared with the LSDA results, we generally find an improved agreement with experiment, since Re $\Sigma^{(2)}$ is positive in the relevant energy range, but has a negative slope, i.e., the shift upwards at lower energies (majority quasiparticles) is larger than at higher energies (minority quasiparticles), and so the difference between the two is reduced. It is interesting to note that the first-order self-energy term alone, i.e., no correlations, produces a large splitting, which is then corrected by the fluctuations; this is similar to the way the Hartree-Fock approximation gives a larger exchange splitting than the one found by using the von Barth–Hedin exchange-correlation potential.[4,5] This effect is also reflected in the larger value for $(U+4J)/5$ relative to I, which includes correlation effects via the exchange-correlation potential (see column 7 in Table II).

It is clear from Figs. 5(a) and 5(b) that the quasiparticles with predominantly $3d$ character become increasingly broad away from the Fermi energy, with surprisingly large values of the full width at half maximum. In actual fact, the maximal full width at half maximum in Fe is nearly as broad as that for Ni, even though the value of U in Fe is a third that of Ni. This is a consequence of the many more possible scattering processes due to

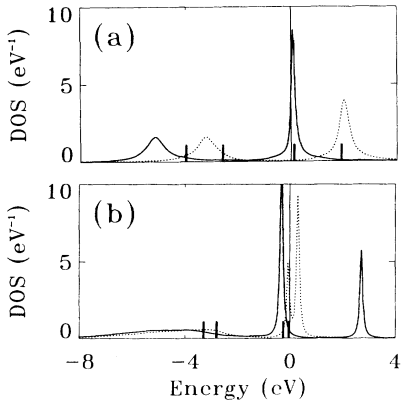

FIG. 5. The spin- and k-resolved DOS for (a) the H point in Fe (with a 0.27-eV broadening) and (b) the X point in Ni. Note that the majority X_2 and X_5 peaks are so close that they cannot be resolved. The solid/dotted lines distinguish between majority/minority states for our results (unbroadened). The thick vertical lines are the positions of the experimental quasiparticles. The energies have been shifted so the Fermi energy is at zero energy.

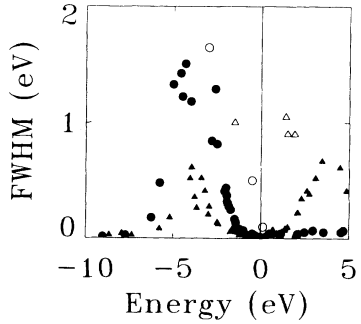

FIG. 6. The full width at half maximum of the quasiparticle peaks in Fe [circles denote majority states, triangles denote minority states, closed symbols denote our results, and open symbols denote experiment (Ref. 12)]. The energies have been shifted so that the Fermi energy is at zero energy.

the creation of minority electron-hole pairs in Fe than in Ni; Fe has a nearly half-filled minority $3d$ band, which is nearly full in Ni. In Fig. 6 the energy dependence of the full width at half maximum of the quasi-particle peaks in Fe (sampled at about 20 k points in the irreducible wedge) is compared with some experimental results. As expected, our values lie below the experimental values, since there are other nonelectronic sources of scattering, such as impurities and phonons, which at the experimental temperature and photon energies also broaden the initial and final states. Near the Fermi energy we have the expected ω^2 behavior for the linewidth, which is suppressed for the majority bands above the Fermi energy because of the essentially filled majority $3d$ bands. A certain amount of broadening is found in the $4s$ and $4p$ bands due to $3d$ to $4s$ and/or $4p$ hybridization.

Although the concept of a quasiparticle is expected to be valid near the Fermi energy, further away in energy the quasiparticle peaks become less well defined and overlap strongly. If the Im $\mathbf{\Sigma}_{k,\sigma}$ is small and the Re $\mathbf{\Sigma}_{k,\sigma}$ smooth, then the roots of the Re[Det($\mathbf{G}^{-1}_{k,\sigma}$)] coincide with the peaks in the Im $\mathbf{G}_{k,\sigma}$. However, often neither is the Im $\mathbf{\Sigma}_{k,\sigma}$ small nor is the Re $\mathbf{\Sigma}_{k,\sigma}$ smooth. All the same, we have found it possible to extract a quasiparticle (or renormalized) band structure for various high-symmetry directions in Fe and Ni, see Figs. 7 and 8. This was done by comparing various combinations of k-resolved partial DOS with the roots of the Re[Det($\mathbf{G}^{-1}_{k,\sigma}$)]. For Co, which has two atoms per unit cell, the broadening is of the order of the band separation over most of the relevant energy range, which makes the resolution of these peaks more difficult. Also plotted are selected experimental results; the triangles are de Haas–van Alphen data, and the circles the position of peaks in the ARPES energy dispersion curves.

Along with the narrowing of the bands and the decrease in the exchange splitting comes an increase in the *quasi*particle DOS at the Fermi energy $g^{\mathrm{QP}}(E_F)$, which is related to the linear specific-heat coefficient γ by $\gamma = (\pi^2/3)k_B^2 g^{\mathrm{QP}}(E_F)$, where k_B is Boltzmann's constant. For the quasiparticle DOS one only needs to know

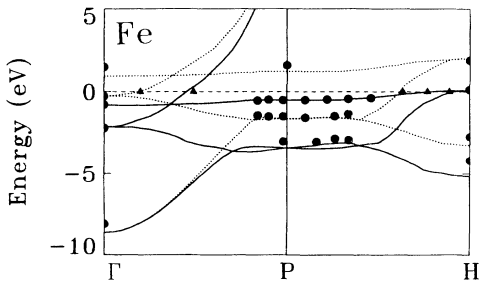

FIG. 7. The quasiparticle band structure of Fe along two symmetry directions (solid/dotted lines are the majority/minority peaks). Also shown are some de Haas–van Alphen (triangles) and selected ARPES results (circles). The energies have been shifted so that the Fermi energy is at zero energy.

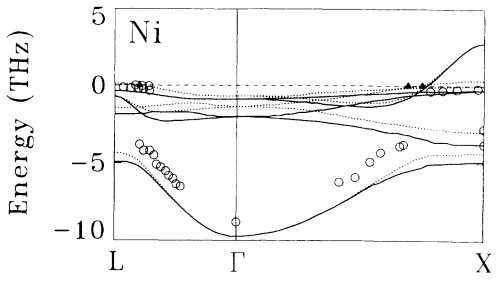

FIG. 8. The quasiparticle band structure of Ni along two symmetry directions (solid/dotted lines are the majority/minority peaks). Also shown are some de Haas–van Alphen (triangles) and selected ARPES results (circles). The energies have been shifted so that the Fermi energy is at zero energy.

the positions of the quasiparticles, while for the normal DOS one also needs to know the weight associated with the peaks. Our results for γ, which are presented in Table I, are enhanced with respect to the LSDA values, and are in reasonable agreement with experimental results, given the uncertainties involved in extracting the purely electronic contribution to the total specific heat.

IV. SUMMARY

In this paper we have further developed a method[1] for improving LDA calculations of the electronic structure of narrow-band, strongly correlated systems. This method assumes that while LDA techniques are adequate for extended metalliclike states, there are important short-range, on-site interactions which need a more sophisticated treatment than is provided by a mean-field approach. We also assumed that these short-range interactions can be modeled by a Hubbard U (and, for magnetic systems, there is a similar on-site exchange term parametrized by J). By calculating perturbatively the self-energy up to second order in the fluctuations induced by U and J around the mean-field LDA solutions, we include dynamic electron-electron correlation effects arising from these short-range interactions, and thus go beyond the mean-field approach.

While the LMTO-ASA method provides good *ab initio* results for the underlying band structure, we have not been able to obtain suitable first-principles results for the Hubbard U, the remaining most important parameter. We have tried several different methods to determine U, but all of these produced rather large values for U, and we therefore empirically determined this value (as well as J) so as to optimize agreement with experimental results for the magnetic moment and the XPS.

The results presented in this paper for the $3d$ transition-metal ferromagnets show that our method leads to significantly better quasiparticle properties, such as effective masses, exchange splittings, and XPS spectra, while leaving practically unchanged ground-state properties, such as partial occupation numbers and the Fermi

surface. Because this new method involves the calculation of a self-energy, it also makes possible calculations of properties such as quasiparticle lifetimes and satellite structure that are beyond the scope of ordinary band theory.

We stress that it is not sufficient to merely include the second-order self-energy, since the chemical potential μ and $\delta n_{m,\sigma}$ must also be consistent with the total number of electrons and with $\langle n_{m,\sigma} \rangle$. Although this substantially increases the computational effort, a direct result in Ni is that, in contrast to earlier work, we simultaneously obtain reasonable agreement at both low and high energies (i.e., the specific-heat enhancements and the satellite).

ACKNOWLEDGMENTS

One of us (M.M.S.) is supported by the University of California's Institutional Collaborative Research (INCOR) program for high-temperature superconductivity. M.M.S. wishes to thank Olle Eriksson and Meb Alouani for many useful discussions. Another (L.J.S.) acknowledges partial support by the National Science Foundation under Grant No. DMR-88-15068, and by the Center for Materials Science, Los Alamos National Laboratory. We acknowledge the supercomputing time provided by the Department of Energy.

APPENDIX A

The basis set used plays an important role in our method. For any given k eigenvector in the mean-field Hamiltonian it is essential to be able to project out the d part of the wave function that is correlated through the U and J first- and second-order self-energy contributions. Moreover, the d-projected occupation numbers (or fillings) directly control the first-order shifts in the quasiparticle energy eigenvalues.

Our starting point is the linearized-muffin-tin-orbital method in the atomic sphere approximation (LMTO-ASA), including the combined-correction terms.[28] This is a reasonable approximation for close-packed systems such as the $3d$ ferromagnets. The $4s$ and $4p$ orbitals are extended and smoothly varying, and should be well treated by LSDA-DFT. The Kohn-Sham eigenvalues for the broad $4s$ and $4p$ bands usually agree well with the experimental quasiparticle energies. For example, the theoretical effective mass of Cu, which has only a slight d-hybridization contribution, agrees well with the purely electronic contribution to the low-temperature specific heat (see Table I), and the $4s$ and $4p$ bandwidths for the $3d$ ferromagnets agree within a few percent, which is well within experimental and theoretical errors (see Santoni and Himpsel[12]). In contrast with the $4s$ and $4p$ orbitals, the $3d$ orbitals are well localized and can easily be associated with a given site. These are the orbitals that are expected to have strong electron-electron correlations.

The basis set that we have used in this paper is based on the LMTO basis set, which therefore makes no constraints on the form of the one-electron hybridization and hopping terms beyond those implicit in the LMTO method itself. Thus, (i) we use the correct crystal and lattice symmetries, and (ii) we use a $3d$, $4s$, and $4p$ basis set on each atom rather then just a $3d$ basis, as is often done. This is important, since the $4s$ and $4p$ to $3d$ hybridization plays an important role in determining the eigenvectors and consequently the $3d$ filling. There is also a segment of the Fermi surface which has a predominantly $4s$ and $4p$ character. We used the von Barth–Hedin approximation for the local exchange-correlation potential.[29]

We can be more explicit about the basis used in this paper and its relationship to the conventional LMTO wave functions, which are a linear combination of linear muffin-tin orbitals for each $\mathbf{k}$ and j. A minor difference between our case and the conventional LMTO is that we use a cubic harmonic basis instead of a spherical harmonic basis and hence our LMTO's are linear combinations of the more conventional ones. Because the LMTO's are not orthogonal, the energy eigenvalue equation has the form $H_{L,L'} - EO_{L,L'} = 0$, where $O_{L,L'}$ is the overlap matrix. One way to define a set of Wannier functions is to do a symmetric transformation of the overlap matrix to reduce this equation to the form $\tilde{H}_{\mu,\nu} - E\delta_{\mu,\nu} = 0$, where the new basis μ and ν is an orthonormal basis that is a linear combination of the original LMTO's. This approach would require a different set of orthonormal (Wannier) functions for each $\mathbf{k}$ point.

For this reason we have chosen a slightly different approach. Our starting point is the LMTO solution for the band wave function, Eq. (4.21a) in Andersen's paper (Ref. 28). Instead of keeping the full wave function, however, we just keep the first term: $\Psi_{j\mathbf{k}} = \sum_L c_L^{jk} \phi_{\nu L}(\mathbf{r})$, where $c_L^{jk} = \sum_{L'} \pi_{LL'}^{\mathbf{k}} A_{L'}^{j\mathbf{k}}$. This is a quite good approximation, with an error in most cases of only a few percent, which we have checked by explicit calculation for the $3d$ ferromagnets. It has the advantage that the basis-set functions $\phi_{\nu L}$ are energy- and $\mathbf{k}$-independent functions, and are therefore in keeping with the spirit of a Wannier functionlike basis set.

The only additional numerical problem is to maintain the orthonormality of the wave functions with respect to the band index j ($\langle \Psi_{jk} | \Psi_{j'k} \rangle = \delta_{j,j'}$), which is only approximately retained [to order $(E - E_\nu)^2 \dot{\phi}^2$, i.e., a few percent] when the second term in the equation for the exact LMTO wave function is dropped. One can ensure this orthonormality by transforming both the Hamiltonian and the overlap, so that the new overlap is the identity matrix. This transformation must be done in a symmetric fashion so as to preserve all the essential symmetries in the original crystal. Thus, in a multisite lattice we must guarantee that the same type of orbital on equivalent atom sites will be the same. To perform this symmetric transformation, we first find the unitary transformation U that diagonalizes the overlap matrix $O_{L,L'} = \sum_j |C_L^j\rangle\langle C_{L'}^j|$ for our approximate wave functions, i.e., $O = U\tilde{O}U^\dagger$, where $\tilde{O}$ is the diagonalized overlap matrix. We can then form $O^{\pm 1/2} = U\tilde{O}^{\pm 1/2}U^\dagger$ by taking the square root or inverse square root of the diagonal elements of $\tilde{O}$. Our orthonormal wave functions are now given by $\tilde{\Psi}_{j\mathbf{k}} = \sum_L \tilde{c}_L^{jk} \phi_{\nu L}(\mathbf{r})$, where $\tilde{c}_L^{jk} = \sum O_{LL'}^{1/2} c_{L'}^{jk}$. The Hamiltonian matrix for our approximate wave func-

tions has elements $H_{L,L'} = \sum_j \epsilon_j |C_L^j\rangle\langle C_{L'}^j|$, where ϵ_j are the energy eigenvalues of the complete LMTO solution. In the orthonormal basis it is transformed so that $\tilde{H} = O^{-1/2} H O^{-1/2}$.

Although partial fillings are always basis-set dependent, in our case, however, the $3d$ orbitals are well localized, and the $3d$ partial fillings are relatively insensitive to this choice of basis. Calculating the projected DOS with our approximate orthonormal functions gives results almost identical with that of the L-dependent projected DOS calculated from the exact LMTO wave functions $\Psi_{j\mathbf{k}}^{\mathrm{LMTO}}$.

The density matrix in this orthonormal basis that is needed in Appendix B will have the form (for L restricted to the d orbitals) $\alpha_{\mathbf{k}\sigma}^{j,L,L'} = \tilde{c}_L^{jk} \tilde{c}_{L'}^{jk\dagger}$.

For the LMTO-ASA calculations we used the Wigner-Seitz radii corresponding to the lattice constants suggested by Papaconstantopoulos.[40] We used the experimental bcc, hcp, and fcc structures for Fe, Co, and Ni, respectively. The charge density was iterated until convergence, using an equally spaced k mesh of about 260 points in the irreducible part of the Brillouin zone.

APPENDIX B

The second-order contribution to the self-energy $\Sigma_{\mathbf{k},\sigma}^{(2)\,dd}$ is calculated in a fashion similar to Ref. 1, except that it is now a 5 by 5 matrix with elements $\Sigma_{\mathbf{k},\sigma}^{m,m'}$, and is biquadratic in U and J, see Fig. 1(f):

$$\Sigma_{\mathbf{k},\sigma}^{m,m'}(\tilde{\omega}) = -\left(\frac{1}{N}\right)^2 \sum_{\substack{k_1,k_2,k_3,K \\ \sigma',m'',m''' \\ j_1,j_2,j_3}} \frac{F_{k_1,k_2,k_3;\sigma,\sigma'}^{j_1,j_2,j_3;m,m',m'',m'''}}{\tilde{\omega} - e_{k_1,\sigma}^{j_1} - e_{k_2,\sigma'}^{j_2} + e_{k_3,\sigma'}^{j_3}} \delta(K + k - k_1 - k_2 + k_3)$$
$$\times \left[f_{k_1,\sigma}^{j_1} f_{k_2,\sigma'}^{j_2} (1 - f_{k_3,\sigma'}^{j_3}) + (1 - f_{k_1,\sigma}^{j_1})(1 - f_{k_2,\sigma'}^{j_2}) f_{k_3,\sigma'}^{j_3} \right],$$

with

$$F_{k_1,k_2,k_3;\sigma,\sigma'}^{j_1,j_2,j_3;m,m',m'',m'''} = U^2 \left(\alpha_{k_1,\sigma}^{j_1,m,m'} \alpha_{k_2,\sigma'}^{j_2,m'',m'''} \alpha_{k_3,\sigma'}^{j_3,m'',m'''} - \delta_{\sigma,\sigma'}\, \alpha_{k_1,\sigma}^{j_1,m,m''} \alpha_{k_2,\sigma}^{j_2,m'',m'''} \alpha_{k_3,\sigma}^{j_3,m''',m'} \right)$$
$$+ JU \left(\alpha_{k_1,\sigma}^{j_1,m'',m'} \alpha_{k_2,\sigma'}^{j_2,m'',m'''} \alpha_{k_3,\sigma'}^{j_3,m,m'''} - \delta_{\sigma,\sigma'}\, \alpha_{k_1,\sigma}^{j_1,m'',m'''} \alpha_{k_2,\sigma}^{j_2,m'',m'''} \alpha_{k_3,\sigma}^{j_3,m,m'} \right)$$
$$+ UJ \left(\alpha_{k_1,\sigma}^{j_1,m,m'''} \alpha_{k_2,\sigma'}^{j_2,m'',m'''} \alpha_{k_3,\sigma'}^{j_3,m'',m'} - \delta_{\sigma,\sigma'}\, \alpha_{k_1,\sigma}^{j_1,m,m'} \alpha_{k_2,\sigma}^{j_2,m'',m'''} \alpha_{k_3,\sigma}^{j_3,m'',m'''} \right)$$
$$+ J^2 \left(\alpha_{k_1,\sigma}^{j_1,m'',m'''} \alpha_{k_2,\sigma'}^{j_2,m'',m'''} \alpha_{k_3,\sigma'}^{j_3,m,m'} - \delta_{\sigma,\sigma'}\, \alpha_{k_1,\sigma}^{j_1,m'',m'} \alpha_{k_2,\sigma}^{j_2,m'',m'''} \alpha_{k_3,\sigma}^{j_3,m,m'''} \right),$$

where the same notation has been used as in Ref. 1, except that $\alpha_{k,\sigma}$ is the 5 by 5 matrix generalization of the $\alpha_{k,\sigma}$ used in Ref. 1, see Appendix A. The term starting with $\delta_{\sigma,\sigma'}$ accounts for the second-order exchangelike diagram, see Fig. 1(f). The band index j_i is preserved along a propagator. However, since the orbital index m is not conserved along a propagator, we have to consider both the on- and off-diagonal elements of $\alpha_{k,\sigma}$. The rest of the calculation of $\Sigma_{\mathbf{k}\sigma}^{(2)\,dd}$ is identical to Ref. 1.

In Ref. 1 the k dependence of the self-energy is written as a Fourier sum. Schweitzer and Czycholl[41] have studied the dependence of the self-energy for the symmetric periodic Anderson model on the number of shells included in the Fourier summation. In strong contrast to the one-dimensional case, they found for a simple cubic lattice in three dimensions that it was only necessary to include up to next-nearest-neighbor shells to obtain a good description of the k dependence. We have checked this shell dependence on Fe and Ni by comparing the results of the Fourier summation at selected k points with those of direct summation over all the bands and both spins, using about 10^6 $\{k_1, k_2, k_3, K\}$ sets under the condition that $K + k - k_1 - k_2 + k_3 = 0$. There is no visible improvement on going to third-nearest-neighbor shell. Even the contribution from the nearest shell is only a few percent of the "local" term. The reasons for this are that not only are the effects of nesting in three dimensions reduced with respect to lower dimensions, but also that in a multiband system there are many more simultaneous possibilities of conserving energy and momentum, which leads to a much weaker k dependence of Im Σ. We mention in passing that the computational effort required to calculate this small k dependence is at least 200 times more than that needed to calculate just the dominant "local" term. On the other hand, both the relative importance of the spin and t_{2g}/e_g orbital dependencies of the self-energy were found to be large in Fe, less so in Co, and small in Ni.

We use Luttinger's sum rule and the Friedel sum rule[42] to speed up the determination of μ and $\delta n_{m,\sigma}$, which have to be consistent with the total number of electrons and with $\langle n_{m,\sigma} \rangle$. At zero temperature Luttinger's sum rule states that the number of electrons in the system is equal to the number of states inside the Fermi surface, which are the solutions of $\mu - \mathbf{H}_k^{\mathrm{MF}} - \Sigma_k(\mu) = 0$ and can be obtained by a single diagonalization at each k point. The Friedel sum rule, the equivalent statement for the partial electron occupations (when generalized to periodic systems), simplifies the calculation of the total and partial

fillings from an energy integration over the Im $\mathbf{G}_{\mathbf{k}\sigma}(\tilde{\omega})$ at each k point to a k-space summation over the well-defined pseudobands and eigenvectors of the Hermitian matrix $\mathbf{H}_k^{\mathrm{MF}} - \mathbf{\Sigma}_k(\mu)$; the k-space summation can be handled by standard methods such as the tetrahedron method. In the final iteration $\mathbf{G}_{\mathbf{k}\sigma}(\tilde{\omega})$ requires a matrix inversion, and the special-ray technique[43] is used for the k summation. A small imaginary term of the order of the energy resolution is added to stabilize the inversion. The k mesh typically has about 300 points in the irreducible part of the Brillouin zone, and the energy mesh discretization is just under 2 mRy.

[1] M. M. Steiner, R. C. Albers, D. J. Scalapino, and L. J. Sham, Phys. Rev. B **43**, 1637 (1991).

[2] P. C. Hohenberg and W. Kohn, Phys. Rev. **136**, B864 (1964); W. Kohn and L. J. Sham, *ibid.* **140**, A1133 (1965); L. J. Sham and W. Kohn, *ibid.* **145**, 561 (1966).

[3] K. B. Hathaway, H. J. F. Jansen, and A. J. Freeman, Phys. Rev. B **31**, 7603 (1985).

[4] C. S. Wang and J. Callaway, Phys. Rev. B **15**, 298 (1977).

[5] R. V. Coleman, W. H. Lowery, and J. A. Polo, Phys. Rev. B **23**, 2491 (1981).

[6] R. W. Godby, M. Schlüter, and L. J. Sham, Phys. Rev. B **37**, 10 159 (1988).

[7] O. Gunnarsson, J. Phys. F **6**, 587 (1976), and references therein.

[8] V. L. Moruzzi, A. R. Williams, and J. F. Janak, Phys. Rev. B **15**, 2854 (1977); *Calculated Electronic Properties of Metals* (Pergamon, New York, 1978).

[9] J. M. MacLaren, D. P. Clogherty, and R. C. Albers, Phys. Rev. B **42**, 3205 (1990).

[10] D. J. Singh, W. E. Pickett, and H. Krakauer, Phys. Rev. B **43**, 11 628 (1991); D. Singh, D. P. Clougherty, J. M. MacLaren, R. C. Albers, and C. S. Wang, *ibid.* **44**, 7701 (1991).

[11] M. B. Stearns, in *Magnetic Properties in Metals*, edited by H. P. J. Wijn, Landolt-Börnstein, New Series, Vol. III, Pt. 19a (Springer, Berlin, 1984); D. Bonnenker, K. A. Hempel, and H. P. J. Wijn, *ibid.*

[12] A. Santoni and F. J. Himpsel, Phys. Rev. B **43**, 1305 (1991); D. E. Eastman, F. J. Himpsel, and J. A. Knapp, Phys. Rev. Lett. **44**, 95 (1980); T. Fauster and F. J. Himpsel, J. Vac. Sci. Technol. A **1**, 1111 (1983); A. M. Turner, A. W. Donoho, and J. L. Erskine, Phys. Rev. B **29**, 2986 (1984); R. Raue and H. Hopster, Z. Phys. B **54**, 121 (1984).

[13] N. E. Phillips, Crit. Rev. Solid State Sci. **2**, 467 (1971); D. A. Papaconstantopoulos, L. L. Boyer, B. M. Klein, A. R. Williams, V. L. Moruzzi, and J. F. Janak, Phys. Rev. B **15**, 4221 (1977).

[14] R. E. Kirby, E. Kisker, F. K. King, and E. L. Garwin, Solid State Commun. **56**, 425 (1985); H. Höchst, A. Goldmann, and S. Hüfner, Z. Phys. B **24**, 245 (1976); Phys. Lett. **57A**, 265 (1976); Z. Phys. B **26**, 133 (1977); M. Lähdeniemi, E. Ojala, and M. Okoochi, Phys. Status Solidi B **108**, K61 (1981).

[15] P. Steiner, S. Hüfner, A. J. Freeman, and D. S. Wang, Solid State Commun. **44**, 619 (1982).

[16] W. Eberhardt and E. W. Plummer, Phys. Rev. B **21**, 3245 (1980).

[17] B. Horvatic and V. Zlatic, Solid State Commun. **54**, 957 (1985); J. Phys. (Paris) **46**, 1459 (1985).

[18] R. N. Silver, J. E. Gubernatis, D. D. Sivia, and M. Jarrell, Phys. Rev. Lett. **65**, 496 (1990).

[19] L. C. Davis and L. A. Feldkampf, Solid State Commun. **34**, 141 (1980).

[20] A. Liebsch, Phys. Rev. Lett. **43**, 1431 (1979); Phys. Rev. B **23**, 5203 (1981).

[21] G. Tréglia, F. Ducastelle, and D. Spanjaard, J. Phys. (Paris) **41**, 281 (1980); **43**, 341 (1982).

[22] L. Kleinman and K. Mednick, Phys. Rev. B **24**, 6880 (1981).

[23] R. G. Jordan and M. A. Hoyland, Solid State Commun. **72**, 433 (1989).

[24] R. Taranko, E. Taranko, and J. Malek, J. Phys. F **18**, L87 (1988); J. Phys. Condens. Matter **1**, 2935 (1989).

[25] N. E. Bickers, D. L. Cox, and J. W. Wilkins, Phys. Rev. B **36**, 2036 (1986).

[26] N. I. Kulikov, M. Alouani, M. A. Khan, and M. V. Magnitskaya, Phys. Rev. B **36**, 929 (1987).

[27] W. Nolting, W. Borgiel, V. Dose, and Th. Fauster, Phys. Rev. B **40**, 5015 (1989); W. Borgiel, W. Nolting, and M. Donath, Solid State Commun. **72**, 825 (1989).

[28] O. K. Andersen, Phys. Rev. B **12**, 3060 (1975); H. L. Skriver, *The LMTO Method* (Springer, New York, 1984).

[29] U. von Barth and L. Hedin, J. Phys. C **5**, 1629 (1972).

[30] B. Brandow, in *Narrow Band Phemonena - Influence of Electrons with Both Band and Localized Character*, edited by J. C. Fuggle *et al.* (Plenum, New York, 1988); V. I. Anisimov, J. Zaanen, and O. K. Andersen, Phys. Rev. B **44**, 943 (1991); M. R. Norman, *ibid.* **44**, 943 (1991).

[31] M. S. Hybertsen, M. Schlüter, and N. E. Christensen, Phys. Rev. B **39**, 9028 (1989), and references therein.

[32] A. K. McMahan, R. M. Martin, and S. Satpathy, Phys. Rev. B **38**, 6650 (1989), and references therein.

[33] O. Gunnarsson, O. K. Andersen, O. Jepsen, and J. Zaanen, Phys. Rev. B **39**, 1708 (1989), and references therein.

[34] B. N. Cox, M. A. Coulthard, and P. Lloyd, J. Phys. F **4**, 807 (1974); J. F. Herbst, R. E. Watson, and J. W. Wilkins, Phys. Rev. B **17**, 3089 (1978); T. Bandyopadhyay and D. D. Sarma, *ibid.* **39**, 3517 (1989).

[35] D. D. Koelling, Rep. Prog. Phys. **44**, 139 (1981).

[36] P. H. Dederichs, S. Blügel, R. Zeller, and H. Akai, Phys. Rev. Lett. **53**, 2512 (1984).

[37] V. I. Anisimov and O. Gunnarsson, Phys. Rev. B **43**, 7570 (1991).

[38] E. Antonides, E. C. Janse, and G. A. Sawatzky, Phys. Rev. B **15**, 1669 (1977); G. Tréglia, M. C. Desjonquères, F. Ducastelle, and D. Spanjaard, J. Phys. C **14**, 4347 (1981).

[39] We have checked the effects of spin-orbit coupling and found them to be small in Ni. Although ASA and full-potential calculations agree well for the LSDA (see Wang and Callaway in Refs. 3 and 4), corrections beyond the LDA such as gradient corrections coupled with the nonspherical terms in a full-potential calculation can give sizable corrections (see Ref. 10). We have also performed calculations starting from the ferromagnetic LMTO solution and find similar results, which further supports our belief that our results are inde-

pendent of the initial choice of the paramagnetic solution as our starting point. However, for systems where the Stoner picture does not hold as well as in the $3d$ ferromagnets, one would not expect such good agreement between the two calculations. The two main differences being in the ferromagnetic calculation: (i) the spin-up and spin-down $4s$ and $4p$ bands are not only indirectly split by hybridization to the $3d$ bands, but also directly by interacting with the exchange-correlation potential, and (ii) J does not have the simple interpretation as the exchange interaction, but rather is a correction to the exchange term in the exchange-correlation potential.

[40] D. A. Papaconstantopoulos, *Handbook of the Band Structure of Elemental Solids* (Plenum, New York, 1986).

[41] H. Schweitzer and G. Czycholl, Solid State Commun. **74**, 735 (1990).

[42] J. S. Langer and V. Ambegaokar, Phys. Rev. **121**, 1090 (1961); R. M. Martin and J. Allen, J. Appl. Phys. **50**, 7561 (1979); R. M. Martin, Phys. Rev. Lett. **48**, 362 (1982).

[43] A. Holas, J. Comput. Phys. **23**, 150 (1977).